Numerical Simulation of Rayleigh-Taylor Instability

A. Sedaghat*
Department of Mechanical Engineering,
Isfahan University of Technology, Isfahan, Iran
E-mail: Sedaghat@cc.iut.ac.ir
*Corresponding author

S. Mokhtarian
Department of Mechanical Engineering,
Isfahan University of Technology, Isfahan, Iran

Received: 13 November 2011, Revised: 19 May 2012, Accepted: 23 July 2012

Abstract: Rayleigh-Taylor (RT) instability has a growing importance in many fields including aircraft industry and astrophysics. The development and the growth of RT instability were investigated using sinusoidal disturbances with different wavelength at the interface of the two fluids. Numerical simulations were performed by solving Navier-Stokes unsteady equations with the VOF formulation. Results of the 2D simulation are compared with experimental results. It is shown that beyond a critical time, not captured experimentally, the mushroom shape of RT instability turns into a helical path or breaks down into a patchy shape depending on the shape of disturbance. Nonlinear instabilities responsible for such behaviour are apparent when the wavelength exceeds 10 times the length scale introduced in this study.

Keywords: Hydrodynamic Instabilities, Multi-Phase Flow, Rayleigh-Taylor

Reference: Sedaghat, A. and Mokhtarian, S. "Numerical Simulation of Rayleigh-Taylor Instability", Int J of Advanced Design and Manufacturing Technology, Vol. 6/ No. 1, 2013, pp. 33-40.

Biographical notes: A. Sedaghat received his PhD in Aerospace Engineering in 1997 from the University of Manchester in UK. He is currently assistant professor at the Department of Mechanical Engineering at Isfahan University of Technology, Isfahan, Iran. His main research interests are in the fields of experimental and computational hydro-aerodynamics and aeroelasticity. **S. Mokhtarian** received his BSc in Mechanical Engineering. He has obtained his MSc in Mechanical Engineering from K.N.T University of Technology, Tehran, Iran. He is interested in vibration of plates.

1 INTRODUCTION

The Rayleigh-Taylor (RT) instability is an important hydrodynamic phenomenon observed when a heavy fluid is accelerated towards a light one [1]. Similar to pouring water into oil, the heavier fluid, once disturbed, streams to the bottom, pushing the light fluid aside. This notion for a fluid in a gravitational field was first discovered by Lord Rayleigh [2] in the 1880s and later applied to all accelerated fluids by Sir Geoffrey Taylor [3] in 1950. Such a density structure arises frequently in many fields including astrophysics [4] and inertial confinement fusion [5].

The RT instability may dramatically reduce the performance of ICF experiments by degrading the symmetry of implosion. In the classical RT experiments, it has been shown that the instability growth is limited by surface tension during the linear stage, where the growth is exponential in time. In ICF experiments the ablation process and the thermal transport are coming into play. The RT growth is stabilized by the flow of material through the ablation front [6]. For both experimental conditions the linear growth rate has a maximum for some wave number.

In atmosphere, temperature fluctuations can occur more frequently under gravitational forces. When the temperature at some point is increased, at constant pressure, the fluid density is lowered. Suddenly, some dense materials are placed on top of some light materials. The Rayleigh-Taylor instability is then initiated which causes an overturn of those layers, thus reassembling the structure.

Rayleigh-Taylor instabilities do not necessarily occur in a gravitational field. A deceleration of a light fluid which encounters a slower heavy fluid may cause the overturn. The general stability conditions of this form were derived by Chandrasekhar [1] in 1981.

Many hydrodynamic instability patterns can be related to a subset of characteristic surfaces of tangential discontinuities. These topological limits, set to systems of hyperbolic PDE's, are locally unstable, but a certain subset associated with minimal surfaces are globally stabilized, persistent and non-dissipative [7-9]. Sections of these surfaces are the spiral scrolls so often observed in hydrodynamic wakes. This method of wake production does not depend explicitly upon viscosity. From the topological point of view it is remarkable how often flow instabilities and wakes take on one or another of two basic scroll patterns.

The first scroll pattern is epitomized by the Kelvin-Helmholtz instability (Fig. 1a) and the second scroll pattern is epitomized by the Raleigh-Taylor instability (Fig. 1b). The repeated occurrence of these two patterns (one similar to a Cornu Spiral and the other similar to a Mushroom Spiral) often deformed but still recognizable and persistent, even in dissipative media, suggests that a basic simple underlying topological principle is responsible for their creation.

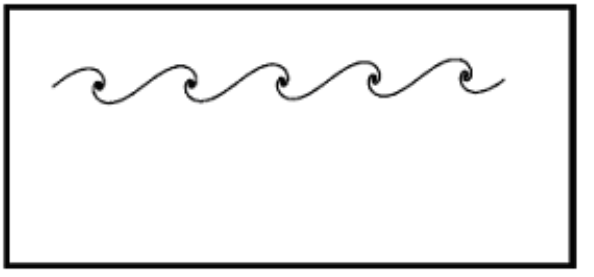

Fig. 1a Pattern of the Kelvin-Helmholtz instability

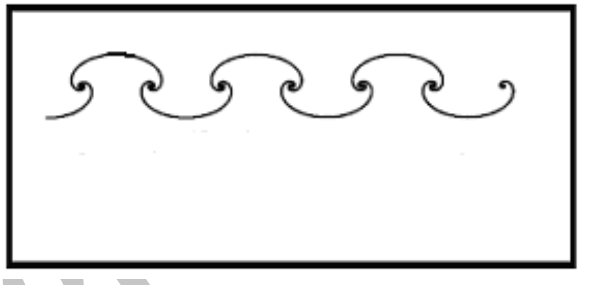

Fig. 1b Pattern of the Rayleigh-Taylor instability

The mushroom pattern is of particular interest because the mushroom pattern appears in many diverse physical systems (in the Frank-Reed source of crystal growth, in the scroll patterns generated in excitable systems, in the generation of the wake behind an aircraft, ...), no simple functional description of the mushroom pattern is given in the literature [7-9]. Classical geometric analysis applied to equations of hydrodynamics has failed to give a satisfactory description of these persistent structures, so often observed in many different situations.

In this paper, the focus is on the interface between two fluids of different densities which exhibit the RT instability, if the light fluid is accelerated into the heavier one as shown schematically in Fig. 2.

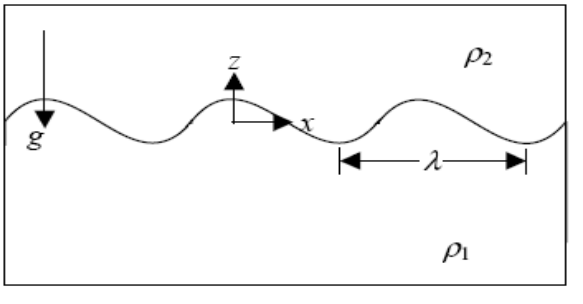

Fig. 2 Schematic of a sinusoidal disturbance at the interface of two constant densities media in a closed chamber

Gravitation or pulsed accelerations induce exponential or linear temporal growth of small sinusoidal disturbances at the interface of two fluids. If the wavelength exceeds certain physical length scale then the instability evolves into the nonlinear stage. Then the flow becomes turbulent and the stage of material mixing will commence.

In this paper, the RT instability problem was formulated on the basis of linear instability theory. As a preliminary research work, numerical simulations were performed by solving RANS unsteady equations. The VOF formulation was incorporated to monitor the development and growth of a sinusoidal disturbance initiated at the interface of two fluids. Results of the 2D simulation of RT instability are presented. The evolution and growth of the interface penetration is closely screened, and the mixing procedure is discussed.

Since linear theory cannot predict the shape of instabilities; further work is required to formulate the effects of nonlinear terms. However, it is shown numerically in this research that when the wavelength exceeds a length scale introduced here, the instability evolves into nonlinear stage. Therefore, the mushroom structure of RT instability turns into a helical path or a patchy structure.

2 FORMULATION OF THE PROBLEM

The Lagrangian equations of continuity and motion for an incompressible, in viscid flow in presence of gravity are, respectively,

$$\frac{\partial \rho}{\partial t} + u \cdot \nabla \rho = 0 \tag{1}$$

$$\rho\left(\frac{\partial u}{\partial t} + u \cdot \nabla u\right) = -\nabla p + \rho g \tag{2}$$

where 'p' is the pressure, 'ρ' is the density, 'u' is the velocity, and 'g' is the gravitational acceleration directed downward as shown in Fig. 2. The pressure and density are assumed stratified and the base flow satisfies the following conditions [10]:

$$p = p(z), \rho = \rho(z), u = 0 \tag{3}$$

Small disturbances for pressure, p', density, ρ', and velocity, u', are introduced as follows:

$$\begin{aligned} p &= p + p' \\ \rho &= \rho + \rho' \\ u &= 0 + u' \end{aligned} \tag{4}$$

Substituting the disturbed quantities from Eq. (4) into the governing fluid flow Eqs. (1) and (2), and ignoring higher order disturbance terms; also subtracting from original Eq. (1), the following disturbance equations are obtained.

$$\frac{\partial(\rho')}{\partial t} = -w\frac{\partial \rho}{\partial z} \tag{5}$$

$$\rho\frac{\partial u}{\partial t} = -\frac{\partial(p')}{\partial x} \tag{6}$$

$$\rho\frac{\partial v}{\partial t} = -\frac{\partial(p')}{\partial y} \tag{7}$$

$$\rho\frac{\partial w}{\partial t} = -\frac{\partial(p')}{\partial z} - g\rho' \tag{8}$$

where (u, v, w) are the (x, y, z) component of the disturbed velocity vector, i.e. u'. Normal modes are introduced for analyzing linear instabilities in the following form.

$$u' = \hat{u}e^{i\left(k_x x + k_y y\right) + st} \tag{9}$$

$$p' = \hat{p}e^{i\left(k_x x + k_y y\right) + st} \tag{10}$$

$$\rho' = \hat{\rho}e^{i\left(k_x x + k_y y\right) + st} \tag{11}$$

Substituting the above normal modes into Eqs. (5)-(8),

$$sp' = -\frac{\partial \rho}{\partial z}w, \tag{12}$$

$$s\rho u = -ik_x p', \tag{13}$$

$$s\rho v = -ik_y p', \tag{14}$$

$$s\rho w = -\frac{\partial(p')}{\partial z} - gp'. \tag{15}$$

By multiplying Eqs. (13) and (14) by k_x and k_y, respectively, and adding the resultant equations,

$$s\rho i(k_x u + k_y v) = (k_x^2 + k_y^2)p' = k^2 p', \tag{16}$$

where $k^2 = k_x^2 + k_y^2$. Substituting the disturbed velocity from Eq. (9) into the continuity equation for incompressible flow, one may obtain:

$$i\left(k_x u + k_y v\right) = -\frac{\partial w}{\partial z}. \tag{17}$$

Thus from Eq. (16),

$$k^2 p' = -s\rho\frac{\partial w}{\partial z}. \tag{18}$$

Now by combining Eqs. (12) and (15) to eliminate ρ' :

$$s\rho w = -\frac{\partial(p')}{\partial z} - \frac{gw}{s}(\frac{\partial \rho}{\partial z}). \tag{19}$$

and using Eqs. (18) and (19) to eliminate p' :

$$\frac{\partial}{\partial z}\left(\rho\left(\frac{\partial w}{\partial z}\right)\right) = k^2\rho w - \frac{gk^2 w}{s^2}\left(\frac{\partial \rho}{\partial z}\right), \tag{20}$$

Considering the conservation equations and also the fact that u and $\frac{\partial w}{\partial z}$ are continuous at the interface boundary, i.e. $z=0$, and by differencing Eq. (18) and integrating Eq. (19) across an infinitesimal segment crossing the boundary, the dynamics boundary conditions may be combined to express a general jump condition:

$$k^2\frac{g}{n}\Delta\left(\rho w\right) = -s\Delta\left(\rho\frac{\partial w}{\partial z}\right), \tag{21}$$

where

$$\Delta f \equiv f(0)_+ - f(0)_- \tag{22}$$

is the jump in quantities across the boundary, and the plus and minus signs denote the limits from the positive and negative sides, respectively. Note that quantities that are continuous across the boundary will have $\Delta f = 0$. Thus,

$$\frac{\partial}{\partial z}\left(\rho\frac{\partial w}{\partial z}\right) = k^2 w\left(\rho - \frac{g}{s^2}\left(\frac{\partial \rho}{\partial z}\right)\right) \tag{23}$$

describes the evolution of fluid after the disturbance, and

$$\Delta\left(\rho\frac{\partial w}{\partial z}\right) = -\frac{gk^2}{s^2}\Delta(\rho w) \tag{24}$$

is the jump condition.

3 EXAMPLE: TWO CONSTANT DENSITY FLUIDS

Taking ρ_1, ρ_2 to be constant and recalling the boundary solution in Eq. (23), one may arrive at an ODE in the form of:

$$\frac{\partial^2 w}{\partial z^2} = k^2 w, \tag{25}$$

which has a general solution in the form of:

$$w = Ae^{(kx)} + Be^{(-kx)}. \tag{26}$$

Employing this into the jump condition Eq. (24) and noting that $w_1(0) = w_2(0)$, one may write:

$$\rho_2\left(\frac{\partial w_2}{\partial z}\right) - \rho_1\left(\frac{\partial w_1}{\partial z}\right) = \frac{-gk^2}{s^2}\left(\rho_2 - \rho_1\right)w_1(0), \tag{27}$$

or using Eq. (25) to yield,

$$-k\rho_2 - k\rho_1 = \frac{-gk^2}{s^2}(\rho_2 - \rho_1), \tag{28}$$

A stability criterion for two superposed, constant-density fluids, are derived by rearranging them to form:

$$s^2 = gkA \tag{29}$$

where

$$A = \left(\frac{\rho_2 - \rho_1}{\rho_2 + \rho_1}\right). \tag{30}$$

'A', is called the Atwood number. It can be seen that for $\rho_2 - \rho_1 > 0$ the solution is temporally unstable because the disturbances expressed in Eqs. (9) to (11) grow in time by positive and real values of '*s*'. The resulting mixing zone is known experimentally [11] to broaden in a way that depends linearly on the gravitational acceleration '*g*', Atwood number, and a quadratic function of time as follows,

$$h = \alpha Agt^2 \tag{31}$$

where '*h*' represent the penetration length, and 'α' has been introduced as a constant of proportionality, sometimes called the acceleration constant. Recent experimental investigations, for 3D cases, give $\alpha \approx .03$ [12].

4 EXPERIMENTAL LITERATURE

Rayleigh-Taylor instability is generated experimentally by accelerating a tank containing the two fluids downward at a rate greater than the earth's gravitational acceleration. The experimental apparatus used at Arizona University [13] consists of a tank that is mounted to a linear rail system and attached by a cable to a weight and pulley system. The bottom half of the tank is filled with a heavy liquid and the top half with a lighter liquid. The filled container is then hoisted to the top of the rail system and then oscillated in the horizontal direction giving the interface a sinusoidal initial perturbation.

The tank is then released allowing the weight to pull it downward at a rate approximately twice that of the earth's gravitational field which produces a net gravitational pull approximately equal to that of the earth's but oriented upward. Thus, the initially stably-stratified system becomes unstable. The fluids are visualized in these experiments [13] using Planar Laser Induced Fluorescence. A fluorescent dye is mixed in one of the liquids and then illuminated with a sheet of laser light passing through the top of the container.

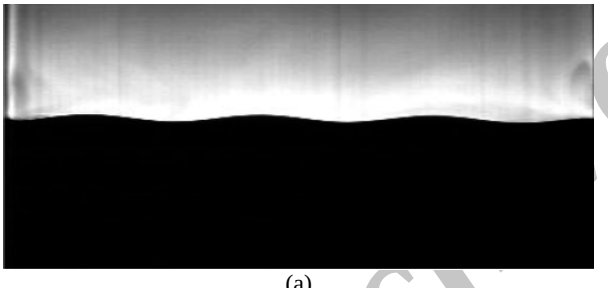

(a)

Fig. 3 (part 1) The behaviour of the fluid interface given an initial sinusoidal disturbance is experimentally shown to be unstable under constant downward acceleration of *g* [8]

The resulting fluorescent images are captured by a CCD camera which travels with the moving container. Pictures in Fig. 3 shows a sequence of images captured during one of these experiments. In these views the effective gravity pulls the lower heavier fluid upward as if the tank had been inverted but without the disrupted effects of actually turning over the tank.

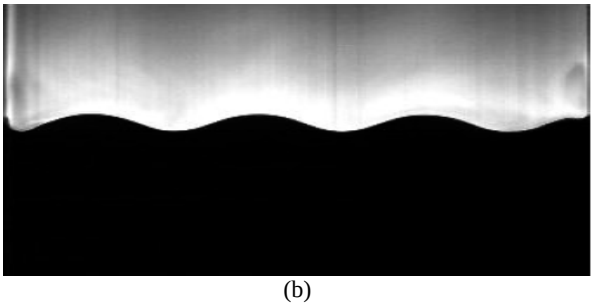

(b)

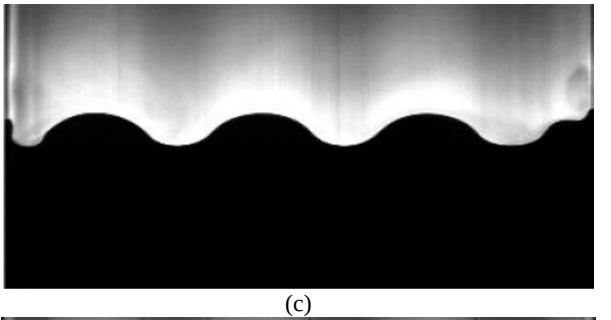

(c)

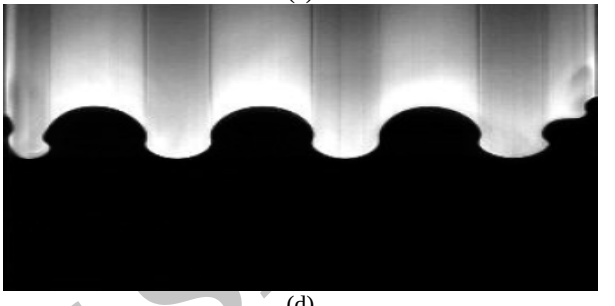

(d)

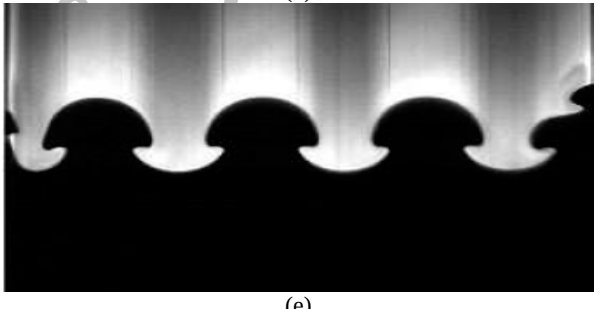

(e)

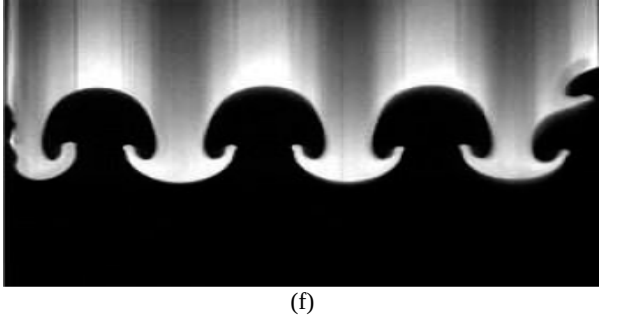

(f)

Fig. 3 (part 2) The behaviour of the fluid interface given an initial sinusoidal disturbance is experimentally shown to be unstable under constant downward acceleration of *g* [8]

5 NUMERICAL SIMULATIONS

In this study, the VOF formulation in FLUENT is used to compute the time-dependent solution for 2D incompressible Navier-Stoks equations [14]. The VOF formulation relies on the fact that two or more fluids (or phases) are not interpenetrating. For each additional phase added to the model, a variable is introduced to the volume fraction of the phase in the computational

cell. In each control volume, the volume fractions of all phases add up to unit volume.
The fields for all variables and properties are shared by the phases and represent volume-averaged values, as long as the volume fraction of each of the phases is known at each location. Thus the variables and properties in any given cell are either purely representative of one of the phases, or representative of a mixture of the phases, depending upon the volume fraction values. In other words, if the q^{th} fluid's volume fraction in the cell is denoted as α_q, then the following three conditions are possible:

$\alpha_q=0$ the cell is empty (of the q^{th} fluid)
$\alpha_q = 1$ the cell is full (of the q^{th} fluid)
$0 < \alpha_q < 1$ the cell contains the interface between the fluids

Based on the local value of α_q, the appropriate properties and variables will be assigned to each control volume within the domain. A rectangular domain as sketched in Fig. 2 was selected as the computational domain. A sinusoidal disturbance was set in the middle of the domain. The surrounding boundaries of the domain were set to solid wall conditions. A structured mesh was generated by Gambit consisting of 240×240 mesh points.

6 RESULTS AND DISCUSSIONS

Numerical results were obtained by solving 2D incompressible Navier-Stokes equation for the rectangular domain with the numerical values for the Atwood number *A=(9/10)* and the total acceleration of *a-g=1.0 (m/s²)*. A sinusoidal disturbance was inserted on the interface of two fluids by defining a length scale as:

$$L^* = \left(\frac{\nu_1^2}{a-g} \right)^{\frac{1}{3}} \quad (32)$$

This length scale was used to determine at what wavelength the nonlinear behaviour of instabilities become more apparent. Dynamics of the development of the disturbed interface in volume fraction is shown in Figs. 4 to 7 from the initial time of 0.0 second to the time of 1.5 second in 0.5 second intervals. The wave length of $\lambda = 5L^*$ was set as the case in which the nonlinear effects are not significant up to a certain time, here 1.0 second.
Simulations agree well with experimental observations as illustrated. The sinusoidal disturbance introduced at the interface of two liquids, is shown in Figure 4. During the first time interval a basic vortex structure forms and develops at the top of the sinusoidal disturbance (Fig. 5), during the second time interval the mushroom shape grows and secondary vortex structures form (Fig. 6), and during the third time interval weak nonlinear terms evolve in time and become evident as secondary vortices appear (Fig. 7). Finally, the formation of nonlinear vortex pattern breaks down into a patchy shape as shown in Fig. 7.

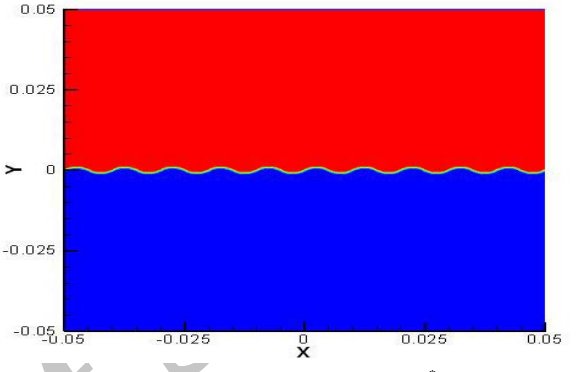

Fig. 4 Sinusoidal disturbance with $\lambda = 5L^*$ at the interface of the heavy fluid (blue) and the lighter fluid (red) at the time of T=0 (sec)

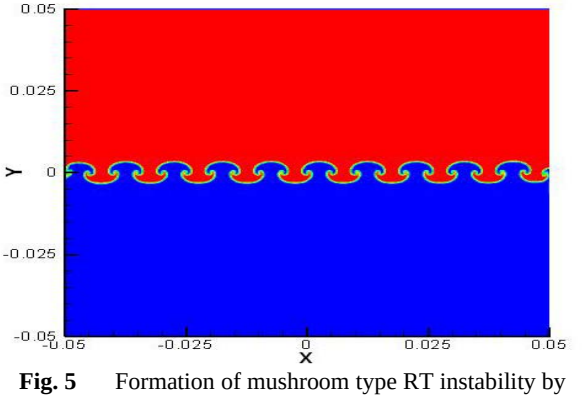

Fig. 5 Formation of mushroom type RT instability by accelerating heavy fluid (blue) into lighter fluid (red) at the time of T=0.5 (sec)

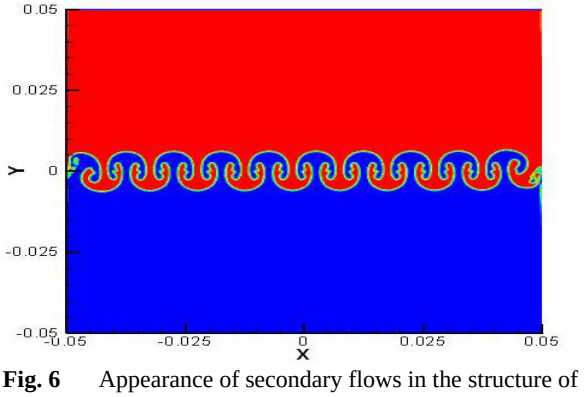

Fig. 6 Appearance of secondary flows in the structure of vortices by further development of the heavy fluid (blue) into lighter fluid (red) at the time of T=1.0 (sec)

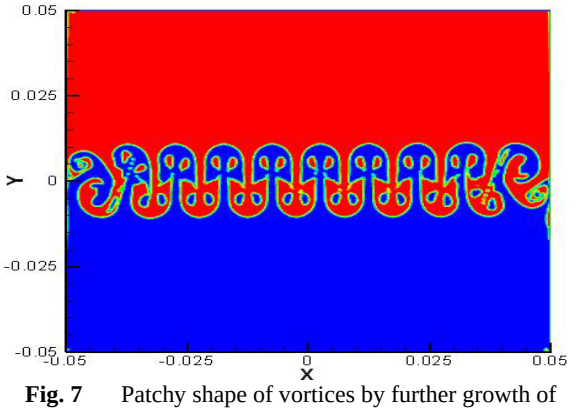

Fig. 7 Patchy shape of vortices by further growth of nonlinear instabilities for accelerating heavy fluid (blue) into lighter fluid (red) at the time of T=1.5 (sec)

Repeating computations with $\lambda = 10L^*$, the development of the disturbed interface is shown in Figures 8 to 12 from the initial time of 0.0 second up to the time of 1.5 seconds with 0.5 second intervals. The sinusoidal disturbance with longer wavelength at the interface of two liquids is shown in Fig. 8.

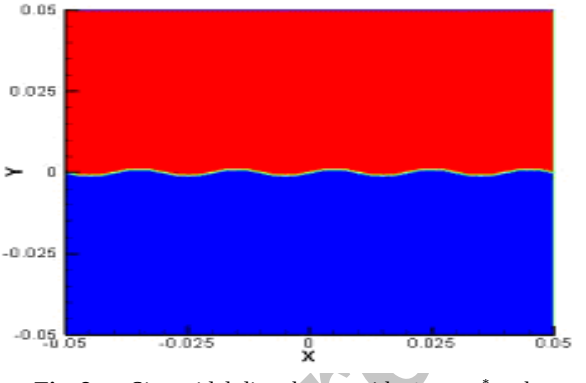

Fig. 8 Sinusoidal disturbance with $\lambda = 10L^*$ at the interface of the heavy fluid (blue) and the lighter fluid (red) at the time of T=0 (sec)

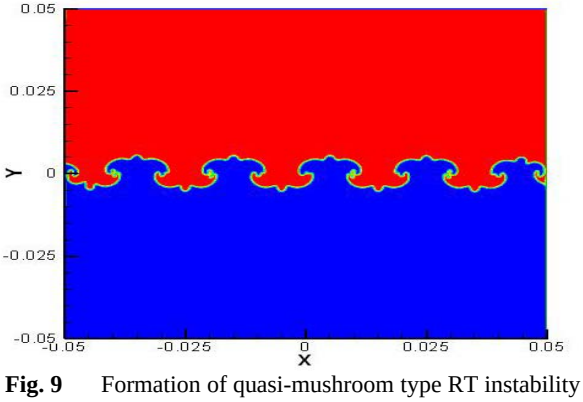

Fig. 9 Formation of quasi-mushroom type RT instability by accelerating heavy fluid (blue) into lighter fluid (red) at the time of T=0.5 (sec)

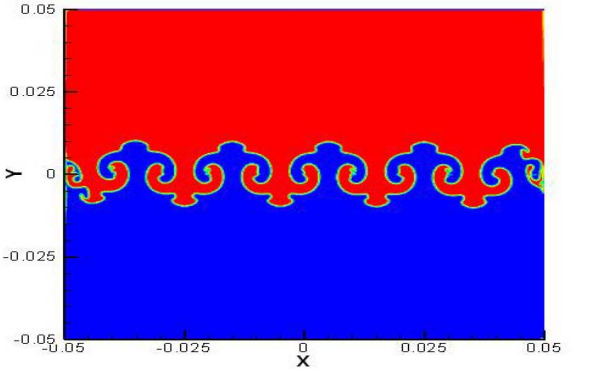

Fig. 10 Further development of the quasi-mushroom type RT instability by accelerating heavy fluid (blue) into lighter fluid (red) at the time of T=1.0 (sec)

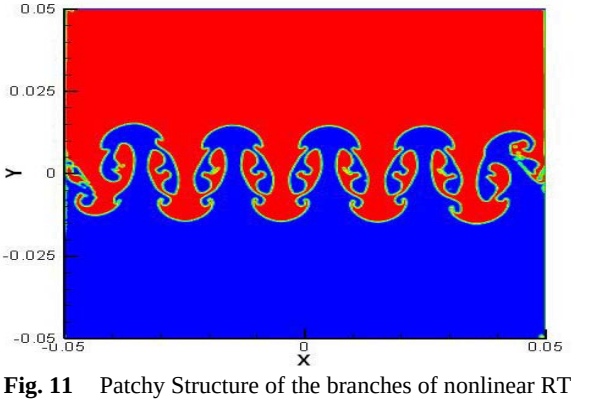

Fig. 11 Patchy Structure of the branches of nonlinear RT instability by accelerating heavy fluid (blue) into lighter fluid (red) at the time of T=1.5 (sec)

The nonlinear effects are significant right at the beginning of development of vortices. During the first time interval a basic quasi-mushroom shape forms and develops at the top of the sinusoidal disturbance (see Figure 9), during the second time interval the quasi-mushroom shape grows into branches (Fig. 10), and finally at the third time interval the stronger nonlinear terms evolve in time and appear as branchy structure of vortices as shown in Fig. 11.

7 CONCLUSION

The mushroom pattern of RT instabilities is of particular interest because it appears in many diverse physical systems such as the wake behind an aircraft. No simple functional description of the mushroom pattern is given in the literature and the classical geometric analysis applied to the equations of hydrodynamics has failed to give a satisfactory description of these persistent structures.

The development and growth of RT instability were investigated using sinusoidal disturbances at the

interface of two fluids with different wavelengths. Numerical simulations were performed by solving Navier-Stokes unsteady equations with the VOF formulation. Introducing a length scale based on the viscosity of fluids and their acceleration, it is shown that nonlinear terms are significant when the wavelength exceeds 10 times the length scale.
Furthermore beyond a critical time, the nonlinear terms become significant and their effects must be considered using nonlinear hydrodynamic instabilities. It is interesting to mention that the shape of initial disturbances may dictate the topological formation and the structure of RT instabilities. This is of current continuing research.

8 ACKNOWLEDGEMENTS

The authors wish to thank Dr. A. R. Pishevar for his critics and proof reading of this article.

REFERENCES

[1] Chandrasekhar, S., "Hydrodynamic and hydromagnetic stability", Dover, 1981, first published by Oxford University Press, 1961.
[2] Rayleigh, L., "100. Investigation of the character of the equilibrium of an incompressible heavy fluid of variable density", Scientific Papers by Lord Rayleigh, Dover, 1964.
[3] Taylor, G., "The instability of liquid surfaces when accelerated in a direction perpendicular to their planes. I", Proceedings of the Royal Society, A, Vol. 202, No. 1066, 1950, pp. 192-196.
[4] Lindl, J. D., "Inertial Confinement Fusion", Springer, New York, 1998.
[5] Haan, S. W., "Weakly nonlinear hydrodynamic instabilities in inertial fusion", Phys. Fluids, B 3, Vol. 3, No. 8, 1991, pp. 2349-2359.
[6] Bodner, S. E., Phys. Rev. Lett., Vol. 33, No. 13, 1974, pp. 761-764.
[7] Kiehn, R. M., "Topological Torsion, Pfaff Dimension and Coherent Structures", in Topological Fluid Mechanics, H. K. Moffatt and A. Tsinober, editors, (Cambridge University Press), 1990, pp. 225.
[8] Kiehn, R. M., "Compact Dissipative Flow Structures with Topological Coherence Embedded in Eulerian Environments", in The Generation of Large Scale Structures in Continuous Media, Singapore World Press, 1991.
[9] Kiehn, R. M., "Topological Defects, Coherent Structures, and Turbulence in Terms of Cartan's theory of Differential Topology", in Developments in Theoretical and Applied Mechanics, SECTAM XVI Conference Proceedings, B. N. Antar, R. Engels, A. A. Prinaris, T. H. Molden. editors (University of Tennessee Space Institute, TN), 1992.
[10] Drazin, P. G., and Reid, W. H., "Hydrodynamic Stability", Cambridge University Press, 1981.
[11] Scheider, M. B., Dimonte, G., and Remington, B., "Large and small structure in Rayleigh-Taylor mixing", Phys Rev.Lett. Vol. 80, 1998, pp. 3507-3510.
[12] Young, Y. N., Tufo, H., Dubey, A. and Rosner, R., "On the miscible Rayleigh-Taylor instability: two and three dimensions", Journal of Fluid Mech, Vol. 447, 2001, pp. 377-408.
[13] The University of Arizona web site, "Rayleigh-Taylor Instability Experiments: http://web.arizona.edu/~fluidlab/rayleigh.html," accessed in 2005.
[14] Peric, P. G., and Reid, W. H., "Hydrodynamic Stability", Cambridge University Press, 1981.